

LETTERS

Compositional homogeneity in the fragmented comet 73P/Schwassmann–Wachmann 3

N. Dello Russo¹, R. J. Vervack Jr¹, H. A. Weaver¹, N. Biver², D. Bockelée-Morvan², J. Crovisier² & C. M. Lisse¹

The remarkable compositional diversity of volatile ices within comets^{1–3} can plausibly be attributed to several factors, including differences in the chemical, thermal and radiation environments in comet-forming regions, chemical evolution during their long storage in reservoirs far from the Sun⁴, and thermal processing by the Sun after removal from these reservoirs. To determine the relevance of these factors, measurements of the chemistry as a function of depth in cometary nuclei are critical. Fragmenting comets expose formerly buried material, but observational constraints have in the past limited the ability to assess the importance of formative conditions and the effects of evolutionary processes on measured composition^{5–8}. Here we report the chemical composition of two distinct fragments of 73P/Schwassmann–Wachmann 3. The fragments are remarkably similar in composition, in marked contrast to the chemical diversity within the overall comet population and contrary to the expectation that short-period comets should show strong compositional variation with depth in the nucleus owing to evolutionary processing from numerous close passages to the Sun. Comet 73P/Schwassmann–Wachmann 3 is also depleted in the most volatile ices compared to other comets, suggesting that the depleted carbon-chain chemistry seen in some comets from the Kuiper belt reservoir is primordial and not evolutionary¹.

Comet 73P/Schwassmann–Wachmann 3 (hereafter 73P) is a Jupiter-family comet that probably originated in the Kuiper belt, on the basis of the short period (5.34 yr) and low inclination (11.4°) of its orbit. Narrowband photometric observations during the 1990 and 2006 apparitions demonstrated that 73P is depleted in C₂ relative to CN and OH (refs 9, 10), placing it in the ‘carbon-chain depleted’ class of comets¹. During its 1995 apparition, the comet split into at least five fragments¹¹, increasing the overall gas production rate by more than an order of magnitude from the previous apparition¹². Observations obtained during the 2006 apparition confirm the disintegration of 73P: 68 named fragments were identified, and at least two of the larger fragments were shedding boulder-sized pieces¹³. Radar observations confirm that the largest fragments (C and B) are of significant size (hundreds of metres in diameter)¹⁴, strongly suggesting that material from different depths (including the deep interior of 73P) is exposed on the surfaces of these bodies.

Jupiter-family comets, although essential for creating a complete chemical taxonomy of comets, are generally too faint for detailed spectroscopic analysis. Thus, they are underrepresented in current surveys, both in number of comets and in detected parent volatiles (species released directly from ices in the nucleus and not products of chemistry in the coma), relative to long-period comets. 73P made a very close approach to Earth in 2006 (Supplementary Table S1), allowing the parent volatile inventory of individual pieces of a fragmenting comet to be determined with unprecedented detail, and

providing a sensitive test for chemical heterogeneity within a comet nucleus.

We measured the volatile composition of the B and C fragments of comet 73P using the Cryogenic Echelle Spectrometer (CSHELL) at the NASA Infrared Telescope Facility¹⁵ (IRTF) and the Near-Infrared Spectrometer (NIRSPEC) at the Keck II telescope¹⁶ on Mauna Kea, Hawaii (Supplementary Table S1). Spectra were acquired between wavelengths (λ) of 2.8 and 4.7 μm at a spectral resolving power sufficient to detect the diagnostic rotational-vibrational lines of parent volatiles in the coma ($\lambda/\Delta\lambda \approx 25,000$). Details of our observing strategy and data processing for both CSHELL and NIRSPEC observations have been given elsewhere^{17,18}. Sample spectra, with the best-fit atmospheric models superimposed, are shown in Fig. 1 (see also Supplementary Figs S1 and S2).

In order to obtain quantitative information from flux-calibrated spectra, the temperature-dependent fluorescence efficiencies (g -factors) for individual rotational-vibrational lines are needed. Fluorescence models have been developed for all sampled parent volatiles^{19–21} (see also Supplementary Information). The measurement of multiple lines with a wide range of ground-state rotational energies enabled the use of these models to determine rotational temperatures for some species (Table 1, Supplementary Fig. S3) using established methodologies¹⁹; otherwise, a reasonable rotational temperature was adopted (Table 1). A sufficient number of both ortho and para H₂O lines were detected to determine ortho-to-para ratios (OPRs) and associated nuclear spin temperatures for both fragments on UT 2006 May 14 and 15. The significance of OPRs is still uncertain, but they may preserve information about conditions in comet-forming regions in the early solar nebula (Supplementary Information). Measurements on both fragments are consistent with the high-temperature statistical equilibrium value of OPR = 3 and spin temperatures greater than 42 and 37 K for 73P-B and 73P-C, respectively (Table 1; see also Supplementary Information).

Integrated column densities for individual lines were extracted using g -factors determined at the measured or adopted rotational temperatures and OPRs, allowing the determination of molecular production rates and relative abundances in 73P-B and 73P-C (Table 1). As might be expected for a fragmenting comet, significant day-to-day variation in absolute production rates was observed, especially for 73P-B. Despite these daily fluctuations in absolute production rates, relative abundances within each fragment remained consistent (Table 1, Fig. 2a). Furthermore, the relative abundances between fragments B and C are remarkably similar to each other when compared to the diversity in chemistry within the overall comet population (Fig. 2b). Given that we are sampling the interior of a recently disrupted comet¹¹, in which layers of increasing depth within the original intact nucleus have been revealed, these results provide strong evidence that the nucleus of 73P is chemically homogeneous

¹Space Department, The Johns Hopkins University Applied Physics Laboratory, 11100 Johns Hopkins Road, Laurel, Maryland 20723-6099, USA. ²Observatoire de Meudon–Paris, LESIA, 5 Place Jules Janssen, Meudon 92190, France.

and that its composition primarily reflects formative conditions and not evolutionary processing.

Earlier infrared observations of 73P acquired in April 2006 reported detections of H₂O in the B and C fragments, and HCN, C₂H₆ and C₂H₂ in the C fragment⁸. Relative abundances in the C fragment from that work agree with those reported here except for C₂H₂. This species was claimed to be several times more abundant than measured upper limits from the present work, and in the normal range of abundances found in the overall comet population⁸—a surprising result, considering that multiple measurements have shown a consistent C₂ depletion in 73P (refs 9, 10). This earlier result might suggest chemical heterogeneity in the nucleus of 73P; however, we regard the detection as unconvincing owing to the relatively low quality of the data and the marginal nature of the reported C₂H₂ detection (Supplementary Information)⁸.

We note that the diversity of formative conditions and processing histories experienced by comets makes it unlikely that the

homogeneous and primitive composition of 73P is representative of all comets. Molecular abundances, presumably from the interior of comet nuclei, have been determined for several fragmenting comets (Supplementary Information). In the case of comet C/2001 A2 (LINEAR), evidence suggests chemical heterogeneity within the nucleus⁷, whereas no conclusive evidence for heterogeneity has been found in other fragmenting comets^{5,6}. Given that 73P and C/2001 A2 (LINEAR) are compositionally different⁷ and are members of

Table 1 | Volatile production rates, abundances, rotational temperatures and OPRs in 73P

Species	UT date (May 2006)	T_{rot}^* (K)	OPR*	T_{spin}^\dagger (K)	Production rate* (10^{25} s^{-1})	Abundance*, H ₂ O = 100
73P/Schwassmann–Wachmann 3-B						
H ₂ O	9.5	120	3.0	>50	3,483 ± 290	
H ₂ O	14.5–14.6	110 $^{+5}_{-3}$	3.2 ± 0.3	>42	1,208 ± 88	
H ₂ O	15.6	98 $^{+4}_{-3}$	3.2 ± 0.3	>42	502 ± 29	
CO	9.5	100			<67 (3 σ)	<1.9 (3 σ)
CH ₃ OH	9.5	100			7.17 ± 1.31	0.206 ± 0.041
CH ₃ OH	14.5	90			2.14 ± 0.29	0.177 ± 0.025
CH ₃ OH	15.6	80			1.70 ± 0.33	0.339 ± 0.066
HCN	9.5	100			8.78 ± 0.80	0.252 ± 0.031
HCN	14.6	87 $^{+5}_{-4}$			3.37 ± 0.34	0.279 ± 0.019
HCN	15.6	73 ± 3			1.44 ± 0.14	0.287 ± 0.015
C ₂ H ₆	9.4	100			4.74 ± 0.54	0.136 ± 0.019
C ₂ H ₆	14.5	127 $^{+40}_{-30}$			1.88 ± 0.28	0.156 ± 0.024
C ₂ H ₆	15.6	80			0.97 ± 0.10	0.193 ± 0.018
H ₂ CO	14.6	100			1.69 ± 0.27	0.140 ± 0.021
H ₂ CO	15.6	100			0.75 ± 0.23	0.15 ± 0.05
NH ₃	9.5	100			<18 (3 σ)	<0.52 (3 σ)
NH ₃	14.5	87			<1.9 (3 σ)	<0.16 (3 σ)
NH ₃	15.6	73			<1.7 (3 σ)	<0.34 (3 σ)
C ₂ H ₂	9.5	100			<3.5 (3 σ)	<0.10 (3 σ)
C ₂ H ₂	14.6	87			0.31 ± 0.13 \ddagger	0.026 ± 0.011
C ₂ H ₂	15.6	73			<0.30 (3 σ)	<0.060 (3 σ)
73P/Schwassmann–Wachmann 3-C						
H ₂ O	3.5	100	3.0	>50	817 ± 98	
H ₂ O	9.6	100	3.0	>50	1,136 ± 154	
H ₂ O	14.5	92 $^{+4}_{-3}$	3.2 ± 0.4	>37	712 ± 48	
H ₂ O	15.6	107 $^{+5}_{-4}$	3.0 ± 0.2	>37	1,090 ± 62	
CO	3.6	80			<21 (3 σ)	<2.6 (3 σ)
CH ₃ OH	14.5	80			1.06 ± 0.21	0.149 ± 0.029
CH ₃ OH	15.6	90			2.77 ± 0.41	0.254 ± 0.037
HCN	9.6	90			3.4 ± 0.9	0.30 ± 0.09
HCN	14.5	77 ± 2			1.72 ± 0.17	0.242 ± 0.014
HCN	15.6	88 ± 3			2.30 ± 0.22	0.211 ± 0.010
C ₂ H ₆	3.5	80			0.53 ± 0.26 \ddagger	0.065 ± 0.033
C ₂ H ₆	9.6	90			1.3 ± 0.4	0.11 ± 0.03
C ₂ H ₆	14.5	88 $^{+24}_{-16}$			0.77 ± 0.08	0.107 ± 0.011
C ₂ H ₆	15.6	100			1.30 ± 0.13	0.119 ± 0.011
H ₂ CO	14.5	100			1.05 ± 0.25	0.147 ± 0.033
H ₂ CO	15.6	100			1.04 ± 0.22	0.095 ± 0.020
NH ₃	14.5	77			<2.4 (3 σ)	<0.33 (3 σ)
NH ₃	15.6	88			<3.2 (3 σ)	<0.29 (3 σ)
C ₂ H ₂	9.6	90			<5.0 (3 σ)	<0.44 (3 σ)
C ₂ H ₂	14.5	77			0.35 ± 0.14 \ddagger	0.049 ± 0.020
C ₂ H ₂	15.6	88			<0.36 (3 σ)	<0.033 (3 σ)

* Calculated rotational temperatures (T_{rot}), ortho-to-para ratios (OPRs), production rates and abundances are listed with error values (± 1 s.e.m.), which incorporate photon noise, calibration uncertainties, and line-by-line deviations between the data and fluorescence models. Values for absolute production rates are sensitive to model assumptions and observing circumstances that are difficult to quantify, including deviations from the spherically symmetric, uniform outflow velocity coma model, errors in the assumed outflow velocity, calibration uncertainties within a setting, uncertainties due to slit losses, temporal variability, and the possible release of volatiles outside our aperture. Therefore, the error bars on absolute abundances may be underestimated. Relative abundances are less sensitive to these factors because most of these species are detected simultaneously within the same grating setting as H₂O (Supplementary Table S1), thereby eliminating most sources of systematic error. T_{rot} and OPR entries with no error bars are adopted values. Rotational temperatures and OPRs were determined within a 3 spectral \times 9 spatial pixel ($0.43'' \times 1.74''$) extract centred on the nucleus.

† Nuclear spin temperatures (T_{spin}) for water are based on calculated OPRs.

‡ Production rates and relative abundances were determined on the basis of positive flux of less than 3 σ using available unblended lines. A positive flux was measured over the two available and apparently unblended ν_3 C₂H₂ lines in both fragments on 14 May. Additional C₂H₂ lines are sampled in this spectral region, but many fall in regions of poor atmospheric transmittance or are probably blended with other species. In addition, coadding weak lines in a spectral region with many emissions (Fig. 1) increases the chance for contamination from unknown or unaccounted for species. Therefore, these 'detections' are not considered firm and are regarded as upper limits. Sample line fluxes and g -factors are given in Supplementary Table S2.

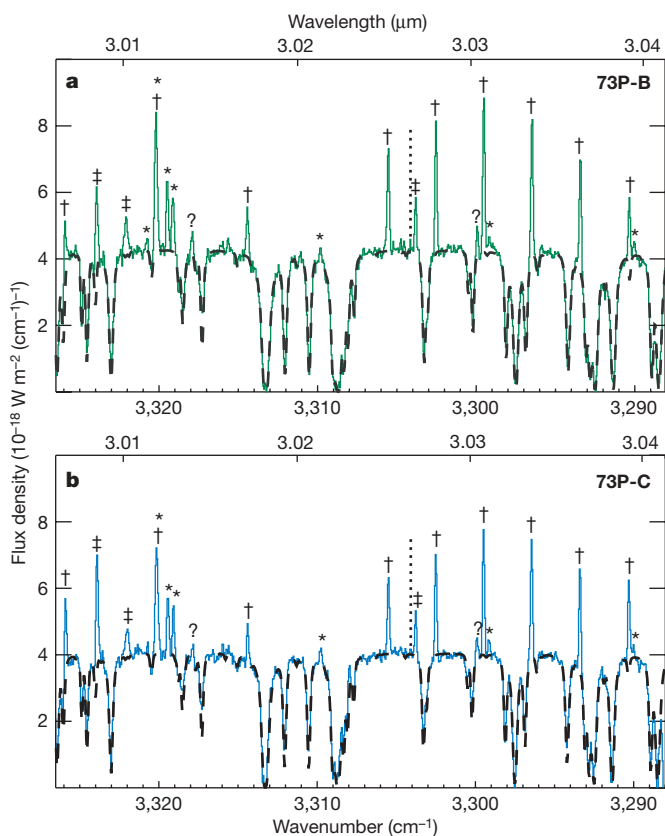


Figure 1 | NIRSPEC spectra of the B and C fragments of comet 73P/Schwassmann–Wachmann 3. Selected high-resolution ($\lambda/\Delta\lambda \approx 25,000$) spectra showing the detection of several species: *H₂O, †HCN, ‡OH, ?unidentified. Spectra are co-added over 3 spectral \times 9 spatial pixel extracts ($0.43'' \times 1.74''$) centred on the peak of the dust continuum. Solid green traces, 73P-B spectra; solid blue traces, 73P-C spectra; and dashed black traces, best-fit synthetic atmospheric models. Molecular lines from the comet are shown as emissions in the comet spectra above the atmospheric model. The 1 σ noise level is $\sim 1 \times 10^{-19} \text{ W m}^{-2} \text{ cm}^{-1}$ in the spectra. Spectral coverage is given in both μm (top) and cm^{-1} (bottom). **a**, 73P-B on UT May 14.6, showing detections of HCN, H₂O and OH (48 min on-source). C₂H₂ emission lines are sampled but are absent in the spectrum. **b**, 73P-C on UT May 15.6, covering the same spectral region as **a** (32 min on-source). Clear detections of HCN, H₂O and OH are seen, but as in **a**, C₂H₂ emissions are absent. The dotted vertical lines near 3,304 cm^{-1} denote the expected position of the strongest unblended C₂H₂ line (ν_3 R3) in both frames. Spectra of the B and C fragments are very much alike (much more similar to each other than to spectra of other sampled comets), and suggest a homogeneous volatile composition for the original intact nucleus of 73P. See also Supplementary Fig. S1.

different dynamical classes, it would not be surprising if their nuclei were structurally dissimilar (homogeneous versus heterogeneous). However, we note that previous measurements of fragmented comets lacked either the sensitivity or the simultaneity of the 73P observations, making interpretation in the same context as the 73P data difficult (Supplementary Information). The extraordinarily favourable

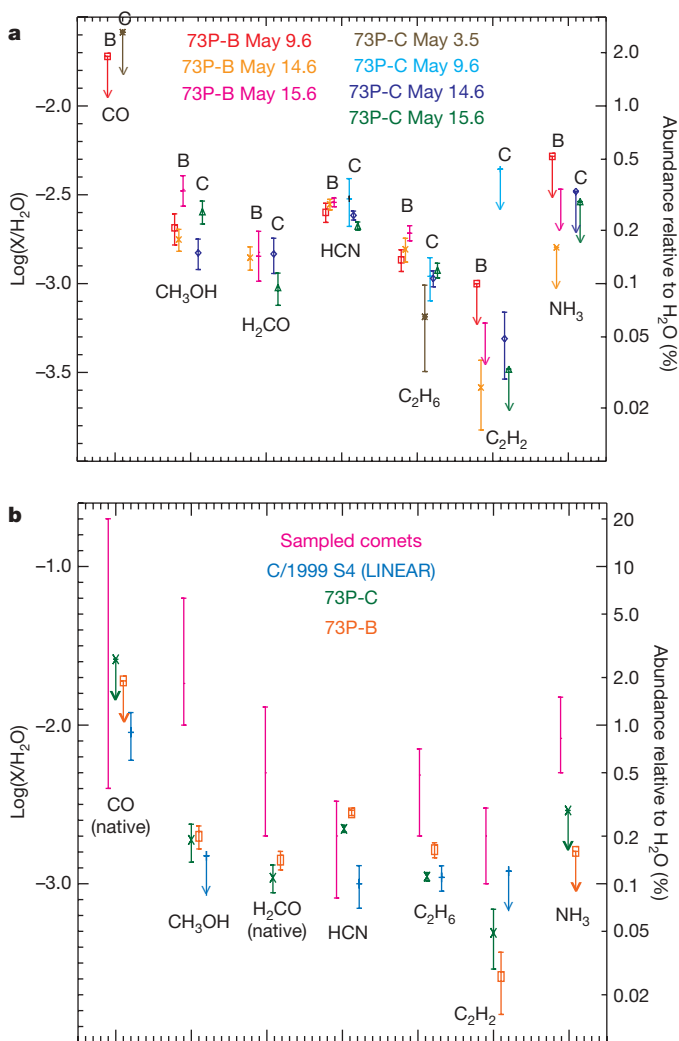


Figure 2 | Relative abundances of detected species in 73P/Schwassmann–Wachmann 3 and comparison to other comets. **a**, Relative abundances for all measured species in 73P/Schwassmann–Wachmann 3. Measurements by date in both fragments B and C are plotted with ± 1 s.e.m error bars (see also Table 1). 3σ upper limits are given by downward arrows. This illustrates that relative abundances are similar from day to day and between fragments. **b**, A comparison of relative volatile abundances in 73P-B and 73P-C, with other comets. The range of measured abundances from the overall comet population (excepting C/1999 S4 (LINEAR)) is denoted by 'Sampled comets'^{22,3}. Abundances for C/1999 S4 (LINEAR) are also plotted³⁰. Relative abundances in 73P represent a weighted average of abundances determined on the dates measured with ± 1 s.e.m error bars. For species that were not detected, the 3σ upper limits are given by downward arrows and represent the most constraining values. For C_2H_2 , the tentative detections from UT May 14.6 are plotted (see Supplementary Information). We note that comparisons of H_2CO (and to a lesser extent CO) in 73P to other comets are complicated by the possible presence of extended sources (see Supplementary Information). This figure illustrates that relative abundances in 73P (with the exception of HCN) resemble those in C/1999 S4 (LINEAR) and are depleted relative to the range of values observed for the general comet population. We note that 73P and C/1999 S4 (LINEAR) are compositionally similar, even though they are from different dynamical classes and probably formed in different nebular regions, further illustrating the difficulties in relating comet chemistry to nebular formation region.

2006 apparition of 73P was unique in that multiple parent volatiles were detected or constrained in two distinct fragments nearly simultaneously with high sensitivity.

Sampling the interior of the Jupiter-family comet 9P/Tempel 1 (hereafter 9P) was a primary goal of the Deep Impact mission²², so a comparison with 73P, also probably from the Kuiper belt reservoir, is desirable. Spacecraft and ground-based analyses of the pre-impact coma and the post-impact volatile ejecta may suggest a heterogeneous composition for 9P (refs 22, 23). Whether the heterogeneity in 9P is due to the accretion of chemically diverse material in the formation epoch or to evolutionary processing with depth is unclear (Supplementary Information). We note that the volatile chemistries of these comets are different; 73P is classified as carbon-chain depleted, whereas 9P is in the carbon-chain normal class (although on the depleted end of normal)¹. This suggests that 73P and 9P experienced different formative conditions or processing histories (or both), despite probably originating from the same reservoir.

Our results also show that in addition to a homogeneous composition, both 73P-B and 73P-C are depleted in all measured volatile species with respect to H_2O , except for HCN (Table 1, Fig. 2, Supplementary Information). Depletion of volatile ices in 73P could indicate that its composition has thermally evolved, even in the deep interior of its nucleus, during numerous perihelion passages; however, modelling studies suggest that thermal processing affects only the outer layers of the nucleus and not the deep interior²⁴. Thermal processing alone also cannot explain why the ratio of CH_3OH to HCN, species with similar volatilities, is about a factor of ten depleted in 73P compared to what is typically seen in comets (Fig. 2b)^{2,3}.

Kuiper belt comets with depleted volatile abundances are common, as more than half of Jupiter-family comets measured with narrowband photometry are in the depleted carbon-chain class¹. In contrast, a significantly smaller fraction (about 20%) of comets depleted in organic volatiles and carbon-chain species have been observed in the long-period Oort cloud population^{1–3}. It has been suggested that these differences are independent of dynamical age, and thus reflect primitive comet chemistry¹. If so, this suggests that Kuiper belt comets formed from source material that was more volatile-poor, on average, than material that accreted into Oort cloud comets. This is counterintuitive, because a colder formation region (the Kuiper belt for Jupiter-family comets versus the giant planets' region for Oort cloud comets) should lead to a higher concentration of the most volatile species in the ices that accreted to form Kuiper belt comets. The distinction between different nebular formation regions, however, is blurred by significant turbulent mixing of materials from the inner and outer solar nebula^{25–27}, as well as by the migration of the giant planets²⁸. If the nebula lifetime was long compared to the time required to accrete comets, the timing of comet formation may rival (or even surpass) the importance of formation region in determining the chemical inventory and structure of cometary nuclei²⁹.

The measured composition of parent volatiles from the deep interior of 73P is consistent with the idea that the depleted carbon-chain chemistry measured in at least some Jupiter-family comets is primordial. However, results suggesting a heterogeneous composition for 9P may indicate that this is not the case for all Jupiter-family comets, and illustrate the difficulty of relating measured comet chemistry to nebular formation region. Whether the timing of comet formation or another as yet unidentified effect primarily causes these differences remains to be seen.

Received 7 March; accepted 2 May 2007.

1. A'Hearn, M. F., Millis, R. L., Schleicher, D. G., Osip, D. J. & Birch, P. V. The ensemble properties of comets: Results from narrowband photometry of 85 comets, 1976–1992. *Icarus* 118, 223–270 (1995).
2. Bockelée-Morvan, D., Crovisier, J., Mumma, M. J. & Weaver, H. A. in *Comets II* (eds Festou, M. C., Keller, H. U. & Weaver, H. A.) 391–423 (Univ. Arizona Press, Tucson, 2005).

3. Biver, N. *et al.* Chemical composition diversity among 24 comets observed at radio wavelengths. *Earth Moon Planets* **90**, 323–333 (2002).
4. Stern, S. A. The evolution of comets in the Oort cloud and Kuiper belt. *Nature* **424**, 639–642 (2003).
5. A'Hearn, M. F., Thurber, C. H. & Millis, R. L. Evaporation of ices from Comet West. *Astron. J.* **82**, 518–524 (1977).
6. Bockelée-Morvan, D. *et al.* Outgassing behavior and composition of comet C/1999 S4 (LINEAR) during its disruption. *Science* **292**, 1339–1343 (2001).
7. Gibb, E. L. *et al.* The organic composition of C/2001 A2 (LINEAR): II. Search for heterogeneity within a comet nucleus. *Icarus* **188**, 224–232 (2007).
8. Villanueva, G. *et al.* The volatile composition of the split ecliptic comet 73P/Schwassmann-Wachmann 3: A comparison of fragments C and B. *Astrophys. J.* **650**, L87–L90 (2006).
9. Fink, U. & Hicks, M. D. A survey of 39 comets using CCD spectroscopy. *Astrophys. J.* **459**, 729–743 (1996).
10. Schleicher, D., Birch, P. V. & Bair, A. N. The composition of the interior of comet 73P/Schwassmann-Wachmann 3: Results from narrowband photometry of multiple components. *Bull. Am. Astron. Soc.* **38**, 485 (2006).
11. Boehnhardt, H. *et al.* 73P/Schwassmann-Wachmann 3 – one orbit after breakup: Search for fragments. *Earth Moon Planets* **90**, 131–139 (2002).
12. Crovisier, J. *et al.* What happened to comet 73P/Schwassmann-Wachmann 3? *Astron. Astrophys.* **310**, L17–L20 (1996).
13. Weaver, H. A. *et al.* Hubble Space Telescope investigation of the disintegration of 73P/Schwassmann-Wachmann 3. *Bull. Am. Astron. Soc.* **38**, 490 (2006).
14. Nolan, M. C. *et al.* Radar observations of comet 73P/Schwassmann-Wachmann 3. *Bull. Am. Astron. Soc.* **38**, 504 (2006).
15. Greene, T. P., Tokunaga, A. T., Toomey, D. W. & Carr, J. B. CSHELL: A high spectral resolution 1–5 μm cryogenic echelle spectrograph for the IRTF. *Proc. SPIE* **1946**, 313–324 (1993).
16. McLean, I. S. *et al.* The design and development of NIRSPEC: A near-infrared echelle spectrograph for the Keck II telescope. *Proc. SPIE* **3354**, 566–578 (1998).
17. Dello Russo, N., DiSanti, M. A., Mumma, M. J., Magee-Sauer, K. & Rettig, T. W. Carbonyl sulfide in comets C/1996 B2 (Hyakutake) and C/1995 O1 (Hale-Bopp): Evidence for an extended source in Hale-Bopp. *Icarus* **135**, 377–388 (1998).
18. Mumma, M. J. *et al.* A survey of organic volatile species in comet C/1999 H1 (Lee) using NIRSPEC at the Keck Observatory. *Astrophys. J.* **546**, 1183–1193 (2001).
19. Dello Russo, N. *et al.* Water production and release in comet 153P/Ikeya-Zhang (C/2002 C1): Accurate rotational temperature retrievals from hot-band lines near 2.9- μm . *Icarus* **168**, 186–200 (2004).
20. Reuter, D. C., Mumma, M. J. & Nadler, S. Infrared fluorescence efficiencies for the ν_1 and ν_5 bands of formaldehyde in the solar radiation field. *Astrophys. J.* **341**, 1045–1058 (1989).
21. Dello Russo, N., Mumma, M. J., DiSanti, M. A., Magee-Sauer, K. & Novak, R. Ethane production and release in comet C/1995 O1 Hale-Bopp. *Icarus* **153**, 162–179 (2001).
22. A'Hearn, M. F. *et al.* Deep Impact: Excavating comet Tempel 1. *Science* **310**, 258–264 (2005).
23. Mumma, M. J. *et al.* Parent volatiles in comet 9P/Tempel 1: Before and after impact. *Science* **310**, 270–274 (2005).
24. Prialnik, D., Benkhoff, J. & Podolak, M. in *Comets II* (eds Festou, M. C., Keller, H. U. & Weaver, H. A.) 359–387 (Univ. Arizona Press, Tucson, 2005).
25. Morfill, G. E. Some cosmochemical consequences of a turbulent protoplanetary cloud. *Icarus* **53**, 41–54 (1983).
26. Bockelée-Morvan, D., Gautier, D., Hersant, F., Huré, J.-M. & Robert, F. Turbulent radial mixing in the solar nebula as the source of crystalline silicates in comets. *Astron. Astrophys.* **384**, 1107–1118 (2002).
27. Lisse, C. M. *et al.* Spitzer spectral observations of the Deep Impact ejecta. *Science* **313**, 635–640 (2006).
28. Levison, H. F. & Morbidelli, A. The formation of the Kuiper belt by the outward transport of bodies during Neptune's migration. *Nature* **426**, 419–421 (2003).
29. Nuth, J. A., Hill, H. G. M. & Kletetschka, G. Determining the ages of comets from the fraction of crystalline dust. *Nature* **406**, 275–276 (2000).
30. Mumma, M. J. *et al.* The startling organic composition of C/1999 S4 (LINEAR): A comet formed near Jupiter? *Science* **292**, 1334–1339 (2001).

Supplementary Information is linked to the online version of the paper at www.nature.com/nature.

Acknowledgements The NASA Planetary Atmospheres and Planetary Astronomy Programs supported this work. Data were obtained at the NASA IRTF operated by the University of Hawaii under cooperative agreement with the NASA Science Mission Directorate, Planetary Astronomy Program. Data were also obtained at the W. M. Keck Observatory, which is operated as a scientific partnership among the California Institute of Technology, the University of California and NASA. The Observatory was made possible by the financial support of the W. M. Keck Foundation. We acknowledge the assistance and expertise of B. Golisch, P. Sears, D. Griep, G. Hill and G. Puniwai, who helped to successfully obtain these data under difficult conditions; and we acknowledge that the summit of Mauna Kea, from which we had the privilege of conducting these observations, is revered within the indigenous Hawaiian community.

Author Information Reprints and permissions information is available at www.nature.com/reprints. The authors declare no competing financial interests. Correspondence and requests for materials should be addressed to N.D.R. (neil.dello.russo@jhuapl.edu).